

Eye Shape and Retinal Topography in Owls (Aves: Strigiformes)

Thomas J. Lisney^a Andrew N. Iwaniuk^c Mischa V. Bandet^b Douglas R. Wylie^{a, b}

^aDepartment of Psychology and ^bCentre for Neuroscience, University of Alberta, Edmonton, Alta., and

^cDepartment of Neuroscience, Canadian Centre for Behavioural Neuroscience, University of Lethbridge, Lethbridge, Alta., Canada

Key Words

Activity pattern · Bird · Eye · Fovea · Habitat · Retinal ganglion cell · Visual streak

Abstract

The eyes of vertebrates show adaptations to the visual environments in which they evolve. For example, eye shape is associated with activity pattern, while retinal topography is related to the symmetry or 'openness' of the habitat of a species. Although these relationships are well documented in many vertebrates including birds, the extent to which they hold true for species within the same avian order is not well understood. Owls (Strigiformes) represent an ideal group for the study of interspecific variation in the avian visual system because they are one of very few avian orders to contain species that vary in both activity pattern and habitat preference. Here, we examined interspecific variation in eye shape and retinal topography in nine species of owl. Eye shape (the ratio of corneal diameter to eye axial length) differed among species, with nocturnal species having relatively larger corneal diameters than diurnal species. All the owl species have an area of high retinal ganglion cell (RGC) density in the temporal retina and a visual streak of increased cell density extending across the central retina from temporal to nasal. However, the organization and degree of elongation of the visual streak varied considerably among species and this variation was quantified using H:V ratios. Species that live in

open habitats and/or that are more diurnally active have well-defined, elongated visual streaks and high H:V ratios (3.88–2.33). In contrast, most nocturnal and/or forest-dwelling owls have a poorly defined visual streak, a more radially symmetrical arrangement of RGCs and lower H:V ratios (1.77–1.27). The results of a hierarchical cluster analysis indicate that the apparent interspecific variation is associated with activity pattern and habitat as opposed to the phylogenetic relationships among species. In seven species, the presence of a fovea was confirmed and it is suggested that all strigid owls may possess a fovea, whereas the tytonid barn owl (*Tyto alba*) does not. A size-frequency analysis of cell soma area indicates that a number of different RGC classes are represented in owls, including a population of large RGCs (cell soma area >150 μm^2) that resemble the giant RGCs reported in other vertebrates. In conclusion, eye shape and retinal topography in owls vary among species and this variation is associated with different activity patterns and habitat preferences, thereby supporting similar observations in other vertebrates.

Copyright © 2012 S. Karger AG, Basel

Introduction

Many features of the eyes of vertebrates show adaptations to the visual environments in which they evolve [Walls, 1942; Hughes, 1977; Lythgoe, 1979; Land and

Nilsson, 2002]. For example, eye shape, defined here as the ratio of corneal diameter (CD) to eye axial length (AL) [Hall and Ross, 2007], varies with differences in activity pattern in terrestrial vertebrates, i.e. reptiles [Hall, 2008], birds [Hall and Ross, 2007; Iwaniuk et al., 2010a; Corfield et al., 2011] and mammals [Kirk, 2004; Ross et al., 2007]. Nocturnal species active under low light intensities generally have a relatively larger cornea and hence high CD:AL ratios. A larger cornea allows for a larger pupil size, which in turn serves to increase the number of photons that reach the retina, thereby improving visual sensitivity [Martin, 1994; Hall and Ross, 2007]. In contrast, diurnal species that are not limited by light availability have eyes with low CD:AL ratios and therefore relatively larger AL and focal lengths. This eye shape is associated with improved spatial resolution. Because focal length determines the size of the retinal area over which the image is spread, increasing this dimension results in increasing the magnification of an image on the retina [Martin, 1982, 1994; Land and Nilsson, 2002]. In turn, this means that each photoreceptor samples a smaller portion of the image compared to an eye with the same photoreceptor dimensions and cell packing but a shorter focal length [Walls, 1942; Martin, 1994; Land and Nilsson, 2002; Kirk, 2004; Hall and Ross, 2007; Hall, 2008].

A second example relates to the relationship between the topographic distribution of retinal ganglion cells (RGCs) across the retina (retinal topography) and habitat. The ‘terrain theory’ of Hughes [1977] suggests that retinal topography is closely related to the symmetry or ‘openness’ of the habitat of a species and there is now considerable evidence from all vertebrate classes to support this view [reviewed by Collin, 1999, 2008]. More specifically, the retinal topography of diurnal species that live in ‘open’ habitats dominated by a horizon (e.g. desert, grassland, ocean floor) is often characterized by an elongated area of increased RGC density stretching across the horizontal retinal meridian, referred to as a visual streak [Hughes, 1977; Collin, 1999, 2008]. Conversely, nocturnal animals and/or species that live in more architecturally complex or ‘enclosed’ habitats (e.g. forests, within coral branches) often lack a distinct visual streak and instead possess a more radially symmetrical arrangement of RGC isodensity contours.

Studies of eye shape in birds [Hall and Ross, 2007; Hall and Heesy, 2010] have largely taken the form of gross comparisons across orders. Such interordinal comparisons yield useful information on broad evolutionary patterns, but whether the same patterns hold true within or-

ders or families is largely unknown [but see Iwaniuk et al., 2010a; Corfield et al., 2011]. In addition, little is known about interspecific variation in retinal topography in birds compared to other vertebrates, especially fishes and mammals [Collin, 1999, 2008; Iwaniuk et al., 2010b]. Here, we specifically examine eye shape and retinal topography within a single avian order, the owls (Strigiformes). Although other avian taxa could also be examined, owls are ideal for such comparisons for two primary reasons. First, unlike many other avian orders, they exhibit variation in both activity pattern and habitat preference [Martin, 1986; Voous, 1988; del Hoyo et al., 1999; König and Weick, 2008] such that comparative analyses can be conducted. Second, much is known about the structure, organization and physiology of the owl visual system. Owls have large, frontally oriented eyes [Oehme, 1961; Fite, 1973; Martin, 1977, 1986; Hall and Ross, 2007; Hall, 2008] characterized by high visual sensitivity [Martin, 1977], poor visual acuity [Fite, 1973; Martin and Gordon, 1974; Harmening and Wagner, 2011] and a higher proportion of rods to cones than other birds [Walls, 1942; Hocking and Mitchell, 1961; Oehme, 1961, 1962; Fite, 1973; Martin, 1982; Braekevelt, 1993; Braekevelt et al., 1996].

Despite this amount of detailed information on owl eyes and the aforementioned variability in activity pattern and habitat, few studies have examined interspecific variation among owls. Oehme [1961] compared the retinas of four owl species and found differences in photoreceptor density, proportion of cones, photoreceptor, interneuron, RGC ratios and fovea shape and depth between three species of primarily nocturnal owl and a more crepuscular species, the short-eared owl (*Asio flammeus*). In another comparison, the diurnal/crepuscular burrowing owl (*Athene cunicularia*) was shown to have a prominent visual streak, a relatively high peak RGC density and a temporal fovea, whereas the nocturnal barn owl (*Tyto alba*) lacks these three features [Bravo and Pettigrew, 1981; Wathey and Pettigrew, 1989]. Murphy and Howland [1983] and Howland et al. [1991] reported substantial interspecific variation in accommodative range among strigid and tytonid owls, which appears to be associated with body size and prey size (smaller owls generally feed on smaller prey). Finally, Lisney et al. [2011] compiled evidence for interspecific variation in rod:cone ratios and critical flicker fusion frequency in owls with different activity patterns, noting that more nocturnally active species have relatively fewer cones and lower critical flicker fusion frequencies compared to species active under higher light intensities.

In this study, we provide a comparison of eye shape and retinal topography across nine species of owl. The species examined represent a range of activity patterns and habitat preferences. As described above, studies on other vertebrate taxa have shown that eye shape and retinal topography vary in a predictable fashion in association with these ecological variables. Therefore, as well as providing detailed descriptions of eye shape and retinal topography in a range of owl species, we specifically predicted that (1) the eyes of diurnal species would exhibit a different eye shape (i.e. a lower CD:AL ratio) compared to nocturnal species, with eye shape in crepuscular species occupying an intermediate position, and (2) species living in open habitats would have a well-defined, elongated visual streak, whereas in species that live in enclosed habitats, the visual streak would be less well defined, showing a more radially symmetrical arrangement.

Materials and Methods

Specimens

Twenty eyes from 12 specimens representing eight species of owl were used in this study. The eyes came from owls collected from wildlife sanctuaries and veterinary clinics, or were donated by other researchers. They were enucleated and immersion-fixed in formaldehyde in 0.1 M phosphate-buffered saline (PBS; pH 7.4) and stored in the same solution at 4°C.

Owls are classified into two extant families: Tytonidae (barn and bay owls) and Strigidae ('typical' owls) [del Hoyo et al., 1999; König and Weick, 2008]. The barn owl is the most studied species with respect to the visual system [see Harmening and Wagner, 2011 for review] and we include one individual in our analyses as a representative tytonid owl. Within the Strigidae, we examined the following seven species: northern saw-whet owl (*Aegolius acadicus*), short-eared owl (*A. flammeus*), snowy owl (*Bubo scandiacus*), great horned owl (*Bubo virginianus*), great grey owl (*Strix nebulosa*), barred owl (*Strix varia*) and northern hawk owl (*Surnia ulula*). Data for the barn owl were also taken from Wathey and Pettigrew [1989], while information for an eighth strigid species, the burrowing owl (*A. cunicularia*), was taken from Bravo and Pettigrew [1981] and Ritland [1982]. This sampling of strigid species encompasses most owl species found within Alberta, Canada (8/11) and includes species from six of the ten Strigiform subfamilies [Wink et al., 2008].

Each species was assigned an activity pattern and habitat category based on information taken from the literature (table 1). Following Hall and Ross [2007], activity pattern was defined as the time of day when the birds are conducting their normal behaviors, and so excludes occasional activities that take place at other times of day. For example, although owls can be classified into discrete activity pattern categories, many species are forced to hunt at any time of day when nesting [Nicholls and Warner, 1972; Tester, 1987; Voous, 1988; Reynolds and Gorman, 1999; König and Weick, 2008]. The three primary activity pattern categories used, (1) diurnal, (2) crepuscular and (3) nocturnal, refer

to species that are primarily active during the day in photopic conditions, during dawn and dusk periods, or at night in scotopic conditions, respectively. Intermediate categories (diurnal/crepuscular and nocturnal/crepuscular) were also used to classify species that are active over two of the three primary categories. A fourth category, cathemeral (meaning a species is equally likely to be active at any time of the 24-hour cycle), was used for the short-eared owl, which was classified as being crepuscular/cathemeral because, although some reports suggest that this species is most active around dawn and dusk [Clark, 1975; Voous, 1988; Reynolds and Gorman, 1999; König and Weick, 2008], others have reported that this owl is active at various times of the day and night [Clark, 1975; del Hoyo et al., 1999]. For statistical analysis (see below), the species classified as showing some degree of crepuscular activity (the burrowing, great grey, great horned and short-eared owls) were combined into one 'intermediate' category ($n = 4$), which was then used for comparison with the nocturnal ($n = 3$) and diurnal ($n = 2$) species. The three habitat categories reflect variation in habitat physical structure. Open habitats, such as tundra, grassland and prairie, are dominated by a horizon and include little vertical structure. In contrast, enclosed habitats, i.e. forests, are physically complex, while the mixed habitat category encompasses species found in either semiopen habitats, such as parkland, or both open and closed habitats.

Eye Shape

Each eyeball was cleaned of all fascia and extraocular muscles before being inflated by injecting a small amount of formaldehyde in 0.1 M PBS with a syringe and small-gauge needle [Hall and Ross, 2007]. The fixative was injected into the eyeball until it was fully inflated and would not accept any more liquid. All 20 eyes could be fully inflated and so were used for subsequent measurements. Maximum CD and maximum eye AL were measured to the nearest 0.01 mm using digital calipers. These values were used to calculate the eye shape, which was defined as the common logarithm (\log_{10}) of the CD:AL ratio [Hall and Ross, 2007].

Retinal Wholemounds

Each eyeball was hemisected and the retina was dissected out of the scleral eyecup. Of the 20 retinas, 15 were of an acceptable condition for wholemounting and were processed further. The retinal pigment epithelial layer could not easily be removed without damaging the retina, hence it was bleached using a solution of 20% hydrogen peroxide in PBS for approximately 24 h at room temperature [adapted from Coimbra et al., 2006]. Each retina was cleared of vitreous, had the pecten cut off at the base and was wholemounted, with the RGC layer uppermost, onto a gelatinized slide coated with Fol's mounting medium [Stone, 1981]. Relieving cuts were made in each retina to enable them to lie flat, and the preparations were then flooded with fresh Fol's medium [Hart, 2002]. Each wholemounted retina was covered with Whatman No. 50 filter paper soaked in 16% paraformaldehyde in PBS. A large coverslip was placed on top of the filter paper and a small weight was applied to the coverslip to ensure that the retina was fixed flat to the slide [Moroney and Pettigrew, 1987; Hart, 2002]. The preparations were stored in a moist chamber for 24 h, after which the weight was removed and each slide briefly washed in distilled water. The wholemounts were then allowed to dry slowly for a number of hours before being defatted in Citrisolv (Fisher Scientific), rehydrated through a descending alcohol series fol-

Table 1. Information on the taxonomy, activity pattern and habitat of each of the nine species of owls used in this study

Family	Species	Common name	Abbreviation	Activity pattern	Symbol	Habitat	Symbol
Strigidae	<i>Aegolius acadicus</i>	northern saw-whet owl	AA	nocturnal	■	enclosed	■
	<i>Asio flammeus</i>	short-eared owl	AF	crepuscular/cathemeral	◻	open	●
	<i>Athene cunicularia</i>	burrowing owl	AC	diurnal/crepuscular	◻	open	●
	<i>Bubo scandiacus</i>	snowy owl	BS	diurnal	◻	open	●
	<i>Bubo virginianus</i>	great horned owl	BV	nocturnal/crepuscular	◻	mixed	◆
	<i>Strix nebulosa</i>	great grey owl	SN	nocturnal/crepuscular	◻	enclosed	■
	<i>Strix varia</i>	barred owl	SV	nocturnal	■	enclosed	■
	<i>Surnia ulula</i>	northern hawk owl	SU	diurnal	◻	mixed	◆
Tytonidae	<i>Tyto alba</i>	barn owl	TA	nocturnal	■	open	●

The species' abbreviations and the symbols denoting activity pattern and habitat are used in figures 2, 5 and 7.

Activity pattern references: Forbes and Warner [1974]; Marti [1974]; Clark [1975]; Hayward and Garton [1988]; Voous [1988]; del Hoyo et al. [1999]; Reynolds and Gorman [1999]; Duncan and Harris [1997]; König and Weick [2008].

Habitat references: Nicholls and Warner [1974]; Forbes and Warner [1974]; Marti [1974]; Clark [1975]; Fast and Ambrose [1976]; Rudolph [1978]; Voous [1988]; del Hoyo et al. [1999]; Duncan [1997]; Duncan and Harris [1997]; Mazur [1997]; König and Weick [2008].

lowed by distilled water and stained for Nissl substance in an aqueous solution of 0.1% cresyl violet (titrated to pH 4.3 with glacial acetic acid). After staining, each retina was rinsed in distilled water and dehydrated through an ascending alcohol series, cleared in Citrisolv and coverslipped with Permount.

Retinal Shrinkage

Using a digital camera (Canon Rebel T1i), scaled photographs of each wholemound were taken before and after staining. The outline of each wholemound pre- and poststaining was traced from the digital images using the public domain NIH image program ImageJ [Rasband et al., 1997–2011] and the percentage of shrinkage was estimated. Shrinkage was low ($7.5 \pm 4.8\%$ on average, \pm SD) and was largely confined to the margins of the wholemound and along the edge of the radial cuts or tears in the distal retina [Stone, 1981]. It was not possible to assess shrinkage caused by primary fixation of the retina in the eyecup, but previous studies suggest this was insignificant [Vaney, 1980; Ehrlich, 1981].

Isodensity Contour Maps and H:V Ratio

Each wholemound was assessed in a systematic random manner using the fractionator concept [Gundersen, 1977]. Digital photomicrographs of the RGC layer were taken at regular intervals defined by a sampling grid measuring between 1×1 and 2×2 mm (depending on wholemound area) using a $\times 100$ oil immersion objective on a Leica DMRE compound microscope with a Retiga EXi Fast Cooled mono 12-bit camera (Qimaging, Burnaby, B.C., Canada) and OPENLAB Imaging system (Improvision, Lexington, Mass., USA). Cells were counted using unbiased counting frames measuring 0.01 mm^2 and consisting of a forbidden line and an acceptance line [Gundersen, 1977] imposed upon each digital photomicrograph using ImageJ. All Nissl-stained cells were counted if they lay within the boundaries of the counting frame or were touching the acceptance line without also

touching the rejection line. Glial cells, which can be distinguished by their elongated 'spindle'- or 'cigar'-like shape and dark staining [Hughes, 1985; Collin and Pettigrew, 1988; Wathey and Pettigrew, 1989; Bailes et al., 2006; Lisney and Collin, 2008] were omitted from the counts. In the highest density, i.e. the perifoveal areas of some of the wholemounds, the cells in the RGC layer were distributed into 2–4 sublayers. For these sample points, digital photomicrographs focused on each sublayer were taken, creating an 'image stack' through the z-axis. Cell counts were then made from each digital photomicrograph in a stack as described above. Care was taken to cross-reference the digital photomicrographs within a stack against each other to avoid double counting. The validity of counts made from the digital photomicrographs was confirmed by viewing the tissue directly under the microscope and making counts while carefully focusing up and down through each sublayer [Bravo and Pettigrew, 1981]. The cell counts for each sample point were entered into a Microsoft Excel spreadsheet and converted to density counts in cells mm^{-2} . The total number of cells in the RGC layer was determined for each retina by multiplying the total number of sampled cells by the inverse of the area sampling fraction, where the area sampling fraction is equal to the area of the counting frame divided by the area of the sampling grid [Howard and Reed, 2005]. For example, for sampling grids measuring 1×1 and 2×2 mm, the resultant area sampling fractions are 0.01 and 0.0025, respectively. Coefficients of error were calculated using the method of Schaeffer et al. [1996] for estimating the coefficients of error of a one-stage systematic sample validated by Glaser and Wilson [1998]. Coefficients of error were less than 0.06 for all the wholemounds, indicating that our total cell number estimates have a high degree of accuracy [Boire et al., 2001; Coimbra et al., 2009; Ullmann et al., 2012].

For each wholemound, the spreadsheet containing the density counts was superimposed upon a scaled outline of the wholemound traced from a digital photograph (see above) created using

Microsoft PowerPoint and was used to identify specialized areas of higher cell density. Additional counts were then made in and around these specialized areas at intervals of 1×1 or 0.5×0.05 mm using the same unbiased counting frame described above. This additional sampling was nonrandom, and so these cell counts were not used in any of the total number of cell estimates. Rather, these counts served to increase our sampling resolution of the higher density areas where the cell gradients are steepest [Stone, 1981; Ullmann et al., 2012], allowing more accurate isodensity contour lines to be drawn (see below). For each wholamount, these additional cell counts were then combined into the existing spreadsheet, which was again superimposed onto the outline of the retinal wholamount as above. Linear interpolation between density counts created isodensity contour lines, which were smoothed by hand [Stone, 1981; Moroney and Pettigrew, 1987; Wathey and Pettigrew, 1989; Hart, 2002; Ullmann et al., 2012], thereby creating an isodensity contour map for each wholamount.

The retinal topography patterns exhibited by each of the wholamounts were quantified by calculating a horizontal:vertical (H:V) ratio [Stone and Keens, 1980]. The H:V ratio is the ratio of the maximum horizontal and vertical extent of the area enclosed by an isodensity contour line [Stone and Keens, 1980; Fischer and Kirby, 1991]. Therefore, a perfectly circular isodensity contour line will have an H:V ratio of 1.0, while increasingly horizontally elongated or 'streaky' [Stone and Keens, 1980] isodensity contour lines will have higher H:V ratios. For each wholamount we calculated the H:V ratio for the four highest cell density isocontours. These four H:V ratios were then averaged to yield a single, average H:V ratio value per species.

Identification of RGCs and Amacrine Cells

As well as the RGCs, glia and a population of so-called displaced amacrine cells are present in the RGC layer in birds as in other vertebrates [Bravo and Pettigrew, 1981; Ehrlich, 1981; Hayes, 1984; Chen and Naito, 1999]. There has been considerable debate in the literature over whether it is possible to distinguish between RGCs and these other cell types in Nissl-stained wholamounts [Hughes, 1977; Stone, 1981; Hughes, 1985]. Some authors recommend erring on the side of caution, suggesting that it is not possible to unequivocally make the distinction between RGCs and other cell types on the basis of morphology and staining characteristics with the exception of glial cells [Hughes, 1985; Collin and Pettigrew, 1988; Wathey and Pettigrew, 1989; Collin and Partridge, 1996; Bailes et al., 2006; Lisney and Collin, 2008]. Following this approach means that the amacrine cell population found in the RGC layer is included in the cell counts. Because the amacrine cells do not contribute an axon to the optic nerve, this means that the cell counts represent an overestimation of the true RGC densities, which may have to be subsequently revised downwards if more specific information becomes available. This approach is given credence because in various vertebrate groups, including fishes, birds (including owls) and mammals, for species for whom the RGC topography has been assessed using both Nissl staining and retrograde labeling from the optic nerve or retinorecipient areas in the brain, both the peak cell densities and the overall topographic distribution of cells remain relatively similar despite the inclusion of the displaced amacrine cells [Bravo and Pettigrew, 1981; Collin, 1988, 1999; Collin and Pettigrew, 1988a; Pettigrew et al., 1988; Chen and Naito, 1999]. Furthermore, because cell

counts from the RGC layer converted to density are then reduced to the square root for the purposes of resolution estimations, the differentiation between RGCs and amacrine cells is not considered to be a major issue [Pettigrew et al., 1988, 2010; Pettigrew and Manger, 2008].

In contrast to this approach, other investigators have advocated the use of cytological criteria to distinguish between RGCs and amacrine cells including a number who have studied avian retinas [Ehrlich, 1981; Hayes and Brooke, 1990; Inzunza et al., 1991; Hart, 2002; Coimbra et al., 2006, 2009; Dolan and Fernández-Juricic, 2010; Fernández-Juricic et al., 2011]. In Nissl-stained material, RGCs are defined as having a relatively large polygonal soma, abundant Nissl substance in the cytoplasm and a prominent nucleolus, while amacrine cells are relatively smaller, have a more circular or 'teardrop' shape and display relatively darker, homogeneous staining [Ehrlich, 1981; Chen and Naito, 1999; Hart, 2002]. We attempted to distinguish between RGCs and amacrine cells in owls using these criteria. In peripheral areas in the majority of the wholamounts it was possible to distinguish between RGCs and amacrine cells, but in the highest density areas this was not possible for two reasons. Firstly, in the high-density areas of avian retinas the RGCs become smaller and increasingly circular/ovoid, thus appearing more like amacrine cells, and the cells themselves overlap considerably [Hayes, 1984; Boire et al., 2001; Hart, 2002; Coimbra et al., 2006]. As was the case with some of the owls, the cells in the highest density areas of avian retinas are often distributed into multiple sublayers [Bravo and Pettigrew, 1981; Moroney and Pettigrew, 1987; Inzunza et al., 1991; Coimbra et al., 2006], further hindering the identification of different cell types in these areas. Secondly, we found that variation in staining intensity across wholamounts meant that differentiating cell types on the basis of their staining properties was not reliable. This variation in staining intensity likely arose from the opportunistic sampling of specimens and associated variation in fixation. To avoid potential issues in differentiating amacrine cells from RGCs, we therefore present retinal topography maps and data based on counts of all Nissl-stained cells as described above.

Cell Soma Area

Each retinal wholamount was divided into three regions on the basis of cell density and location: (1) 'low' densities ($<10,000$ cells mm^{-2}) in the retinal periphery, (2) 'medium' densities ($10,000$ – $20,000$ cells mm^{-2}) in the visual streak and (3) 'high' densities ($>20,000$ cells mm^{-2}) in the temporal retina. The barn owl wholamounts were only divided into two regions (of low and medium density) because of the lower cell densities observed in this species compared to the strigid owls. Two-dimensional areal measures of cell soma area were made for at least 400 cells from randomly selected digital photomicrographs using ImageJ for each region.

Statistical Analysis

Variation in eye shape and H:V ratio in relation to activity pattern and habitat was tested using nonparametric Kruskal-Wallis tests. As mentioned above, for activity pattern, the four species classified as showing some degree of crepuscular activity were combined into one intermediate category ($n = 4$), and compared against the nocturnal ($n = 3$) and diurnal ($n = 2$) species. We also used hierarchical cluster analysis performed on the eye shape and three retinal topography variables, peak cell density, centropo-

ripheral density gradient and H:V ratio, which are particularly important for defining differences in retinal topography between different groups of animals [Hughes, 1977]. The data used in the cluster analysis were all standardized on a scale of 0–1 prior to analysis [Quinn and Keough, 2002] and the analysis was undertaken using PAST software [Hammer et al., 2001]. Retinal topography variables such as AD, CD and others were not included because they were used to derive the variables of interest and/or are highly correlated, meaning they would be overrepresented in the cluster analysis [Mooi and Sarstedt, 2011]. Comparing cluster dendrograms with a phylogeny of the species of interest can reveal whether interspecific variation is largely attributable to phylogenetic relatedness or to some ecological or behavioral factor(s) [Iwaniuk and Hurd, 2005]. This approach has been widely used in comparative studies of avian neuroanatomy [Rehkamper et al., 2003; Iwaniuk and Hurd, 2005; Iwaniuk et al., 2006; Gutiérrez-Ibáñez et al., 2011], including studies on the visual system [Partridge, 1989; Hart, 2001]. We compared cluster dendrograms to the owl phylogeny studied by Wink et al. [2008], which represents the most complete molecular phylogeny for owls currently available. Only the dendrogram produced using Ward's linkage is presented, but the dendrograms arising from other linkage methods (e.g. UPGMA, single linkage) were of a similar topology.

Results

Eye Shape

Eye shape varied considerably among the species examined (table 2; fig. 1). The northern saw-whet owl occupies one end of the spectrum with the largest cornea relative to AL (fig. 1a) and an average \log_{10} (CD:AL) ratio of -0.140 . In contrast, the northern hawk owl has a noticeably smaller cornea relative to AL (fig. 1d) and a CD:AL ratio of -0.226 . All the other species lie between these two extremes, as illustrated by the short-eared owl and the great grey owl, which have average CD:AL ratios of -0.171 and -0.190 , respectively (fig. 1b, c). For the three species for which 3 or more eyes were available for measurement (the northern saw-whet, great horned and barn owls), the standard deviations are relatively small, indicating that eye shape is consistent between individuals within a species (table 1; fig. 2). There is some evidence that interspecific variation in eye shape corresponds with activity pattern, but not habitat preference (fig. 2). The three nocturnal species (the barn, northern saw-whet and barred owls) have amongst the highest CD:AL ratios, whereas the diurnal species (the snowy and northern hawk owls) have the lowest ratios (fig. 2a). The four species have exhibited some degree of crepuscular activity (the burrowing, great grey, great horned and short-eared owls) and have intermediate CD:AL ratios, although the CD:AL ratios for the diurnal/crepuscular burrowing owl and the crepuscular/cathemeral short-eared owl are clos-

Table 2. Eye AL, maximum CD (both measured in mm) and eye shape (Shape) values for nine species of owl used in this study

Species	Eye 1	Eye 2	Eye 3	Eye 4	Eye 5	Averages ± SD
Northern saw-whet owl						
AL	18.1	16.4	16.4	16.4	16.7	16.8 ± 0.7
CD	13.2	11.9	11.5	12.4	11.9	12.2 ± 0.7
Shape	-0.138	-0.139	-0.154	-0.121	-0.147	-0.140 ± 0.01
Short-eared owl						
AL	18.9	18.2				18.6
CD	13.2	11.9				12.5
Shape	-0.157	-0.185				-0.171
Burrowing owl						
AL	17.0 ^a					17.0
CD	11.6 ^a					11.6
Shape	-0.166					-0.166
Snowy owl						
AL	36.7	36.3				36.5
CD	21.6	22.4				22.0
Shape	-0.230	-0.210				-0.220
Great horned owl						
AL	35.5	34.3	35.7	34.5	34.6	34.9 ± 0.6
CD	22.7	22.8	23.6	23.8	23.5	23.3 ± 0.5
Shape	-0.194	-0.177	-0.180	-0.161	-0.168	-0.176 ± 0.01
Great grey owl						
AL	25.4					25.4
CD	16.4					16.4
Shape	-0.190					-0.190
Barred owl						
AL	27.8	28.5				28.2
CD	19.4	20.0				19.7
Shape	-0.156	-0.154				-0.155
Northern hawk owl						
AL	19.7					19.7
CD	11.7					11.7
Shape	-0.226					-0.226
Barn owl						
AL	18.8	18.2	19.0 ^b			18.5 ± 0.4
CD	13.1	13.0	13.5 ^b			13.1 ± 0.1
Shape	-0.157	-0.146	-0.148			-0.152 ± 0.01

^a From Ritland [1982].

^b From Wathey and Pettigrew [1989].

er to those found in the nocturnal species. Comparing eye shape between nocturnal, intermediate and diurnal species statistically (fig. 2a) yielded a significant difference among the three groups (Kruskal-Wallis $\chi^2 = 7.00$, $p = 0.03$). There was, however, no significant difference in eye shape among the three habitat categories (Kruskal-Wallis $\chi^2 = 2.41$, $p = 0.30$) (fig. 2b).

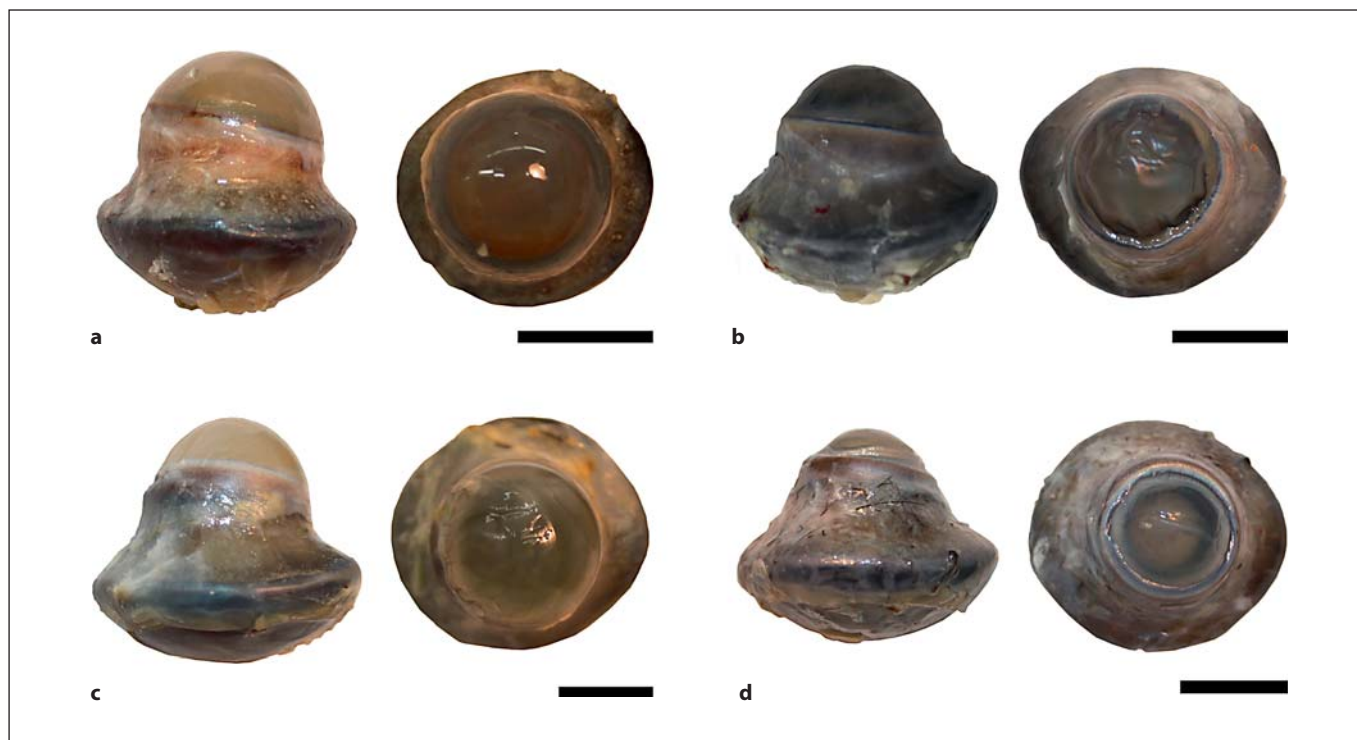


Fig. 1. Dorsal and side views of excised eyeballs from four species of owl. **a** Northern saw-whet owl. **b** Short-eared owl. **c** Great grey owl. **d** Northern hawk owl. Each eyeball has been fully inflated with fixative, as described in Materials and Methods, allowing eye AL and maximum CD to be measured. Scale bars represent 10 mm.

Retinal Topography and H:V Ratio

The density of cells in the RGC layer varied across the retina in all eight species (fig. 3). The cells were distributed in a discrete single layer except in the highest density areas where 2–4 sublayers of cells could be identified in five of the eight species, but not in the northern saw-whet, short-eared and barn owls. Isodensity contour maps showing the species-specific distributions of cells in the RGC layer (fig. 4) reveal that all the owl species possess an area of high cell density in the temporal retina. In seven of the eight species, plus the burrowing owl [Bravo and Pettigrew, 1981], a fovea was positively detected in this part of the retina (table 3; fig. 3, 4). In all the owls, a visual streak stretching from the temporal retina towards the central or nasal retina was present; however, the organization of the visual streak varies among species. Some owls, particularly the snowy owl but also the short-eared and northern hawk owls, have a well-defined visual streak characterized by closely packed isodensity contour lines (fig. 4a–c). In other species, notably the barred, northern saw-whet and barn owls (fig. 4g–i), the visual streak is more poorly defined, with the isodensity

contour lines being more loosely packed and displaying a more radially symmetrical arrangement. Such a retinal topography pattern is sometimes referred to as a ‘weak visual streak’ [Bailes et al., 2006; New and Bull, 2011]. The three remaining species, the burrowing, great horned and great grey owls, display an intermediate condition (fig. 4d–f). This interspecific variation in the retinal topography pattern was quantified by calculating average H:V ratios for each species (table 3). For the two species for which three wholemounts were available (the great horned and barn owls), the standard deviations are relatively small, indicating that H:V ratio, like eye shape, is consistent among individuals within a species (table 3; fig. 5). The H:V ratio in owls appears to vary with both activity pattern and habitat (fig. 5). The three nocturnal species have H:V ratios ≤ 1.46 , whereas the two diurnal species have H:V ratios ≥ 2.78 (fig. 5a). Species that show some degree of crepuscular activity have correspondingly intermediate H:V ratios, ranging between 1.77 and 2.92. When we compared the nocturnal, intermediate and diurnal species, there was a significant difference in H:V ratio (Kruskal-Wallis $\chi^2 = 6.30$, $p = 0.04$) (fig. 5a).

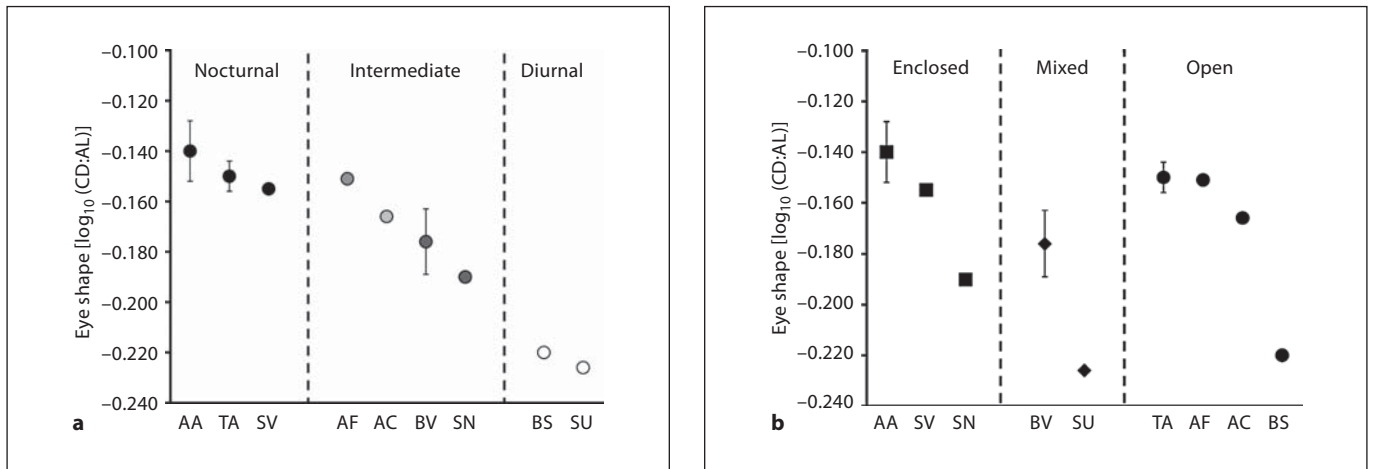


Fig. 2. Variation in eye shape in owls in relation to activity pattern (**a**) and habitat (**b**). Average values are plotted for each species, and for species for which three wholemounts were measured \pm standard deviations are presented. Following table 1, the species names are abbreviated and the variation in the shading and the shape of the symbols reflects the activity pattern and habitat pref-

erence of each owl species, respectively. **a** The species are grouped according to activity pattern (nocturnal, intermediate, diurnal), following the approach used for the nonparametric statistical analysis outlined in Materials and Methods. **b** The species are grouped according to habitat (enclosed, mixed, open).

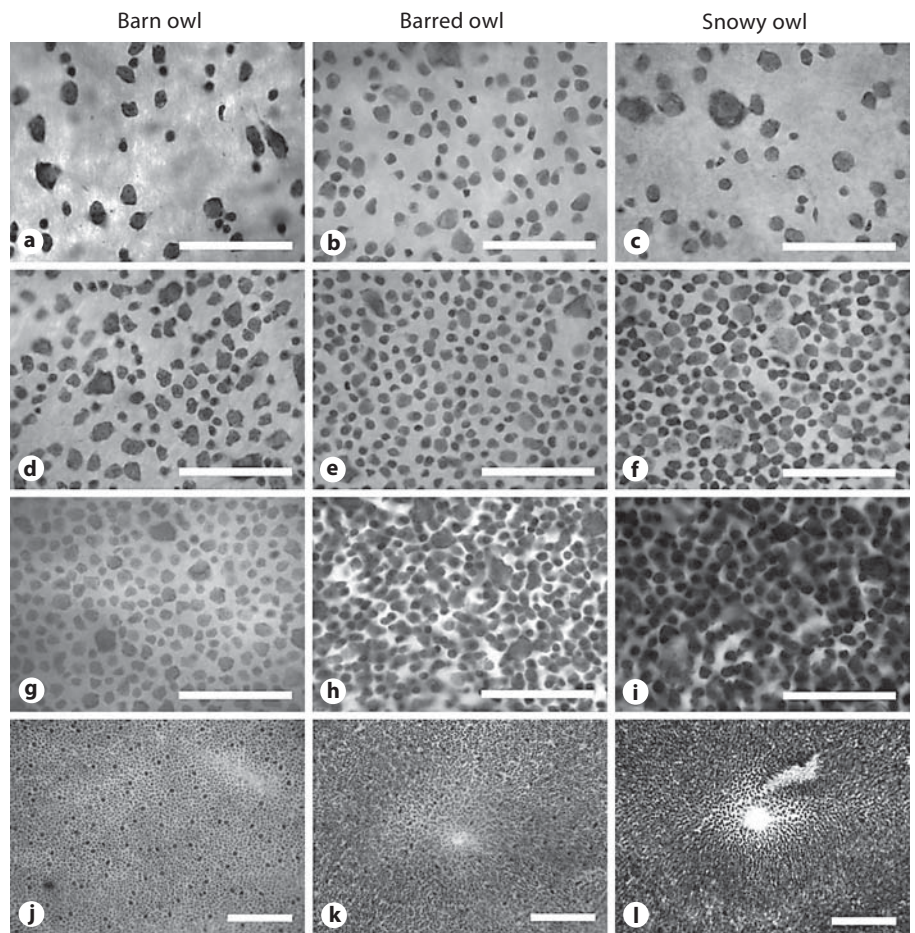


Fig. 3. Nissl-stained cells in the RGC layer in three species of owl, the barn owl (**a, d, g, j**), the barred owl (**b, e, h, k**) and the snowy owl (**c, f, i, l**). High-power ($\times 100$ objective) digital photomicrographs illustrate cells in low- (**a–c**), medium- (**d–f**) and high-density (**g–i**) regions of the retina. Lower-power ($\times 20$ objective) digital photomicrographs show the area of peak cell density or area centralis in the barn owl, located in the epicenter of the image (**j**), and fovea in the barred (**k**) and snowy owls (**l**). Scale bars represent $50 \mu\text{m}$ (**a–i**) and $150 \mu\text{m}$ (**j–l**).

Table 3. Summary of retinal topography data in nine species of owl

Species	Eye	Poststain wholemount area, mm ²	Total number of cells in the RGC layer	Peak cell density cells mm ⁻²	Lowest cell density cells mm ⁻²	Average cell density cells mm ⁻²	Centroperepheral density gradient	H:V ratio	Fovea identified
Northern saw-whet owl	1	217.4	1,917,000 (0.032)	25,233	4,730	8,18	5.3	1.11	yes
	2	182.2	1,979,200 (0.030)	28,000	4,800	10,863	5.8	1.75	no
	average	199.8	1,948,100	26,617	4,765	9,841	5.6	1.43	yes
Short-eared owl	1	271.7	2,437,200 (0.028)	22,480	4,227	8,970	5.3	2.72	yes
	2	237.2	2,465,200 (0.030)	22,230	4,417	10,393	5.0	3.11	yes
	average	254.5	2,451,200	22,355	4,322	9,682	5.2	2.92	yes
Burrowing owl	1	358.7 ^a	–	23,000 ^b	<5,000 ^c	–	5.1 ^d	2.50 ^a	yes
Snowy owl	1	599.3	5,973,200 (0.059)	34,313	3,400	9,967	10.1	4.03	yes
	2 ^e	774.6	–	34,000	3,400	–	10.0	3.72	yes
	average	687.0	5,973,200	34,157	3,400	9,967	10.1	3.88	yes
Great horned owl	1	1,060.0	7,060,400 (0.042)	25,950	3,890	6,734	6.7	2.85	no
	2	729.1	7,059,600 (0.032)	27,500	3,700	9,683	7.4	2.10	yes
	3	1,110.3	6,454,000 (0.037)	25,000	2,000	5,813	12.5	2.05	yes
	average	962.6 ± 204.6	6,858,000 ± 349,874	26,150 ± 1,262	3,197 ± 1,041	7,410 ± 2,002	8.9 ± 3.2	2.33 ± 0.45	yes
Great grey owl	1	400.0	5,313,825 (0.029)	29,080	3,798	13,285	7.7	1.77	no
Barred owl	1	533.4	7,150,800 (0.033)	35,283	7,716	13,406	4.6	1.38	yes
	2	618.2	6,679,600 (0.033)	31,833	4,350	13,406	7.3	1.58	yes
	average	575.8	6,915,200	33,558	6,053	12,105	6.0	1.48	yes
Northern hawk owl	1	481.5	5,920,425 (0.025)	29,433	6,500	13,855	4.5	2.78	yes
Barn owl	1	230.7	1,223,900 (0.041)	19,080	3,750	5,305	5.1	1.24	no
	2	193.3	1,319,000 (0.037)	18,760	3,173	6,824	5.9	1.29	no
	3	336.0 ^f	1,400,000 ^f	12,500 ^f	<2,000 ^g	–	6.6 ^h	1.02 ⁱ	no
	average	253.3 ± 74.0	1,314,300 ± 88,144	16,780 ± 3,710	3,462	6,065	5.5	1.27 ± 0.14	no

Values for individual eyes and average values are presented, along with ± standard deviations for the two species for which data for 3 eyes were available. The coefficients of error for the estimates of total numbers of cells in the retinal ganglion cell layer are given in parentheses in the relevant row.

^a Measured with ImageJ using the isodensity contour map presented in Bravo and Pettigrew [1981].

^b From Bravo and Pettigrew [1981].

^c The value of the lowest isodensity contour on the isodensity contour map presented in Bravo and Pettigrew [1981] is 5,000 cells mm⁻².

^d Calculated assuming conservatively that the lowest cell density is 4,750 cells mm⁻², which is 5% lower than the lowest isodensity contour presented in Bravo and Pettigrew [1981].

^e It was not possible to sample the entire right snowy owl wholemount in a systematic random manner, so there is no estimate of the total number of cells for this wholemount.

^f From Wathey and Pettigrew [1989].

^g The value of the lowest isodensity contour on the isodensity contour map presented in Wathey and Pettigrew [1989] is 2,000 cells mm⁻².

^h Calculated assuming conservatively that the lowest cell density is 1,900 cells mm⁻², which is 5% lower than the lowest isodensity contour presented in Bravo and Pettigrew [1981].

ⁱ Measured with ImageJ using the isodensity contour map presented in Wathey and Pettigrew [1989].

This reflects the much larger H:V ratios in diurnal compared to nocturnal species. With respect to habitat, there is a trend for species that live in enclosed habitats to have lower H:V ratios (1.43–1.77) compared with species found in open or mixed habitats (H:V ratios >2). The exception to this trend is the barn owl, which lives in open habitats but has the lowest average H:V ratio (1.18). We detected no statistically significant differences in H:V ratio among the 3 habitat types (Kruskal-Wallis $\chi^2 = 2.40$, $p = 0.30$). However, when the barn owl was excluded from the anal-

ysis, the difference approached significance (Kruskal-Wallis $\chi^2 = 5.56$, $p = 0.06$).

Numbers and Densities of Cells in the RGC Layer

Quantitative information on the numbers and densities of cells in the RGC layer for each species is presented in table 3. The average total number of cells in the RGC layer was estimated to range from 1,314,300 in the barn owl to 6,915,200 in the barred owl. Average cell densities ranged from 6,064 cells mm⁻² in the barn owl to 13,855

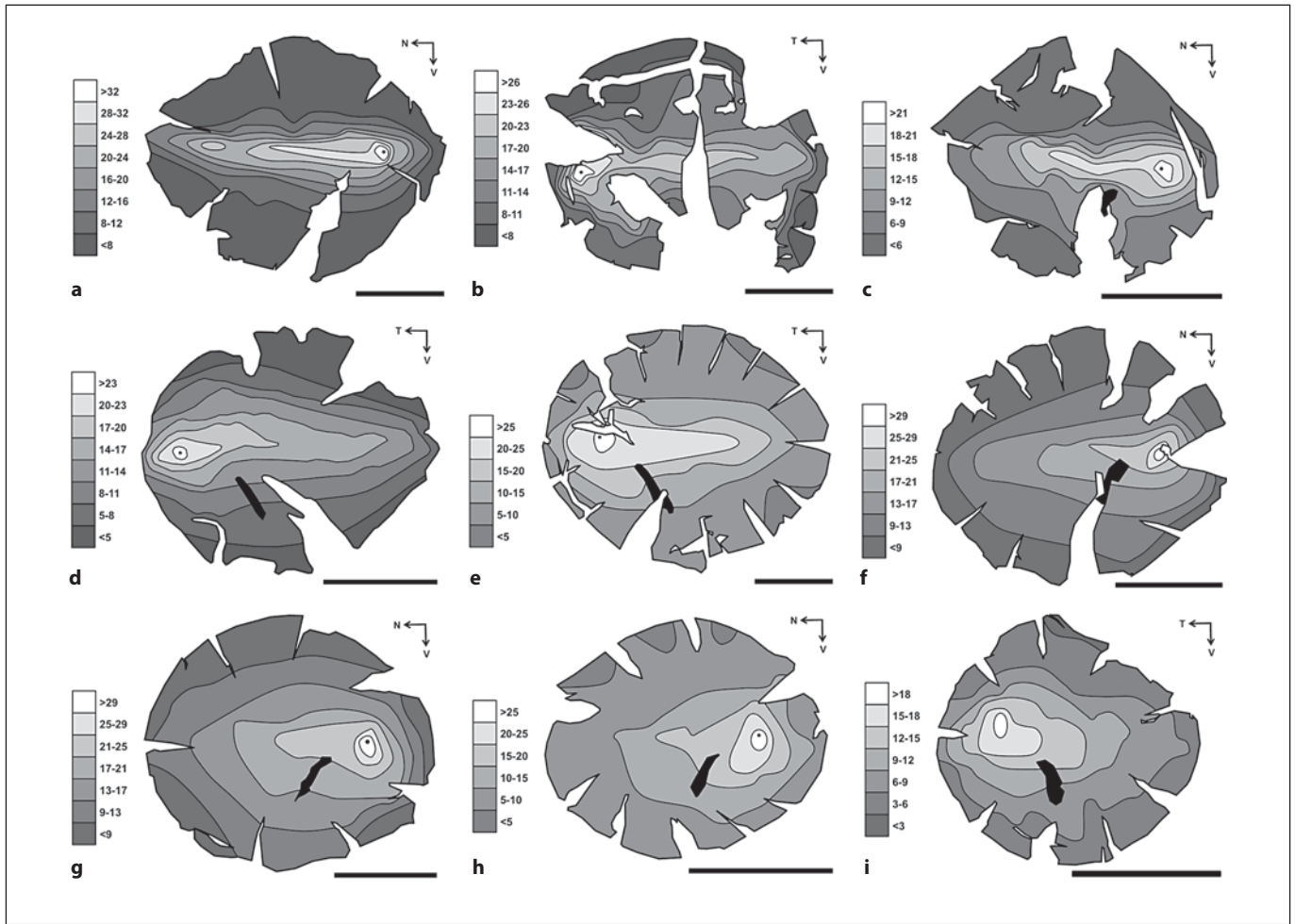


Fig. 4. Retinal topography in owls. **a–h** Isodensity contour maps of cells in the RGC layer for nine species of owl. **a** Left retina from the snowy owl. **b** Right retina from the northern hawk owl. **c** Left retina from the short-eared owl. **d** Right retina from the burrowing owl [redrawn from Bravo and Pettigrew, 1981]. **e** Right retina from the great horned owl. **f** Left retina from the great grey owl. **g** Left retina from the barred owl. **h** Left retina from the northern saw-whet owl. **i** Right retina from the barn owl. All nine species

exhibit a temporal area of high cell density and in seven species a fovea was positively identified, as indicated by a small black dot in the highest density contour. The shaded density scales, which are different between species, represent $\times 10^3$ cells mm^{-2} . The irregular black shapes in **c–i** represent the position of the pecten. Scale bars represent 10 mm. N = Nasal; T = temporal; V = ventral.

cells mm^{-2} in the northern hawk owl. In all species, the peak cell densities were in the temporal area (in the perifoveal region in species where a fovea was detected), and average peak cell densities ranged from 16,780 cells mm^{-2} in the barn owl to 34,157 cells mm^{-2} in the snowy owl. The lowest average cell densities in peripheral areas ranged from 3,197 cells mm^{-2} in the great horned owl to 6,583 cells mm^{-2} in the northern hawk owl. Finally, average centroperipheral gradients in cell density ranged from 4.5:1 in the northern hawk owl to 10:1 in the snowy owl.

Cell Soma Size-Frequency Distributions

A comparison of cell soma area was made for three retinal regions (areas of low, medium and high density) in the eight species that we examined directly. In all species, a predominantly unimodal distribution of cell sizes was identified, and the soma size frequency histograms for low-, medium- and high-density regions of each retina reveal a positively skewed distribution with cell soma area varying from approximately 12 to 360 μm^2 (fig. 6). The peak size frequency was typically centered between 20 and 40 μm^2 in all of the histograms. In all species, a

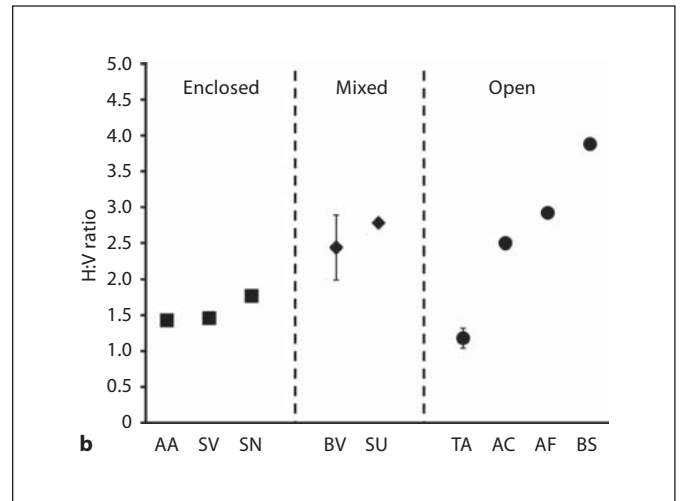
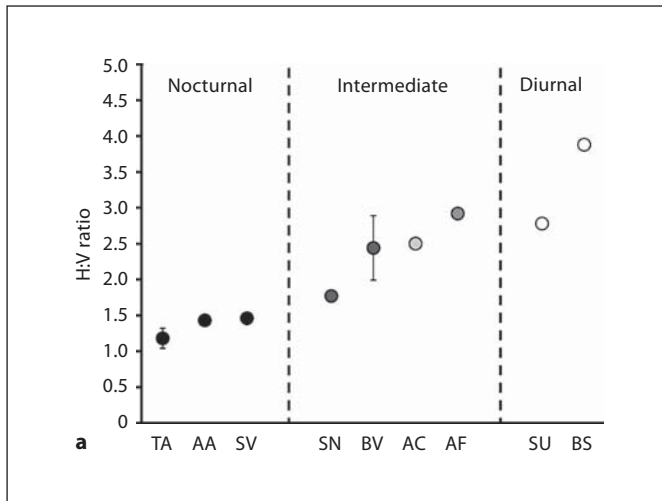


Fig. 5. Variation in H:V ratio in owls in relation to activity pattern (a) and habitat (b). Average values are plotted for each species, and for species for which three wholemounts were measured \pm standard deviations are presented. Following table 1, the species names are abbreviated and the variation in the shading and the shape of the symbols reflects the activity pattern and habitat preference of each owl species, respectively. The species are grouped as in figure 2.

small number of large ($>150\text{--}360\ \mu\text{m}^2$) cells were identified. Because of the skewed frequency distributions, the small number of large cells distorts the average cell soma area values for each species. Therefore, median values, which are more resistant to extreme values within a sample, are presented instead. In all species the median cell soma area was inversely proportional to cell density. The overall median cell soma area for each species ranged from $24.7\ \mu\text{m}^2$ in the northern saw-whet owl to $35.8\ \mu\text{m}^2$ in the barn owl (fig. 6).

Multivariate Analysis

Three clusters were identified in the hierarchical cluster analysis dendrogram based on eye shape and three retinal topography variables (fig. 7a). A comparison of this dendrogram with the owl phylogeny (fig. 7b) reveals that the clustering of species does not reflect phylogenetic relationships, but rather species that share activity patterns and to a lesser extent habitat preferences are clustered together. The only diurnal species that lives predominantly in open habitats included in this analysis, the snowy owl, is separated from all other species. The second ‘cluster’ of species is the most varied, containing the diurnal northern hawk owl, the crepuscular/cathemeral short-eared owl and the diurnal/crepuscular burrowing owl, species that live in open or mixed habitats. Finally, the five nocturnal/crepuscular and nocturnal species are grouped together

in the third cluster. Within this cluster there is some separation between the two nocturnal/crepuscular species, the great horned and great grey owls, and the three nocturnal species, the barn, northern saw-whet and barred owls. All five of these owls live in enclosed or mixed habitats, with the exception of the barn owl.

Discussion

Although this study represents the most detailed comparison of eye shape and retinal topography both within an avian order and across a range of owl species, there are potential caveats that need to be considered when interpreting the results. Our access to owl tissue was limited

Fig. 6. Cell soma area (μm^2) vs. % frequency histograms of cells located in low- ($<10,000\ \text{cells mm}^{-2}$), medium- ($10,000\text{--}20,000\ \text{cells mm}^{-2}$) and high- ($>20,000\ \text{cells mm}^{-2}$) density regions of the RGC layer in eight species of owl. At least 400 cells were measured in each of the three retinal regions for each wholemount, and for species where more than one wholemount was analyzed the data for each wholemount were combined. The overall median soma area \pm 95% confidence limits is provided for each species, along with the median soma area (med) \pm 95% confidence limits for each retinal region.

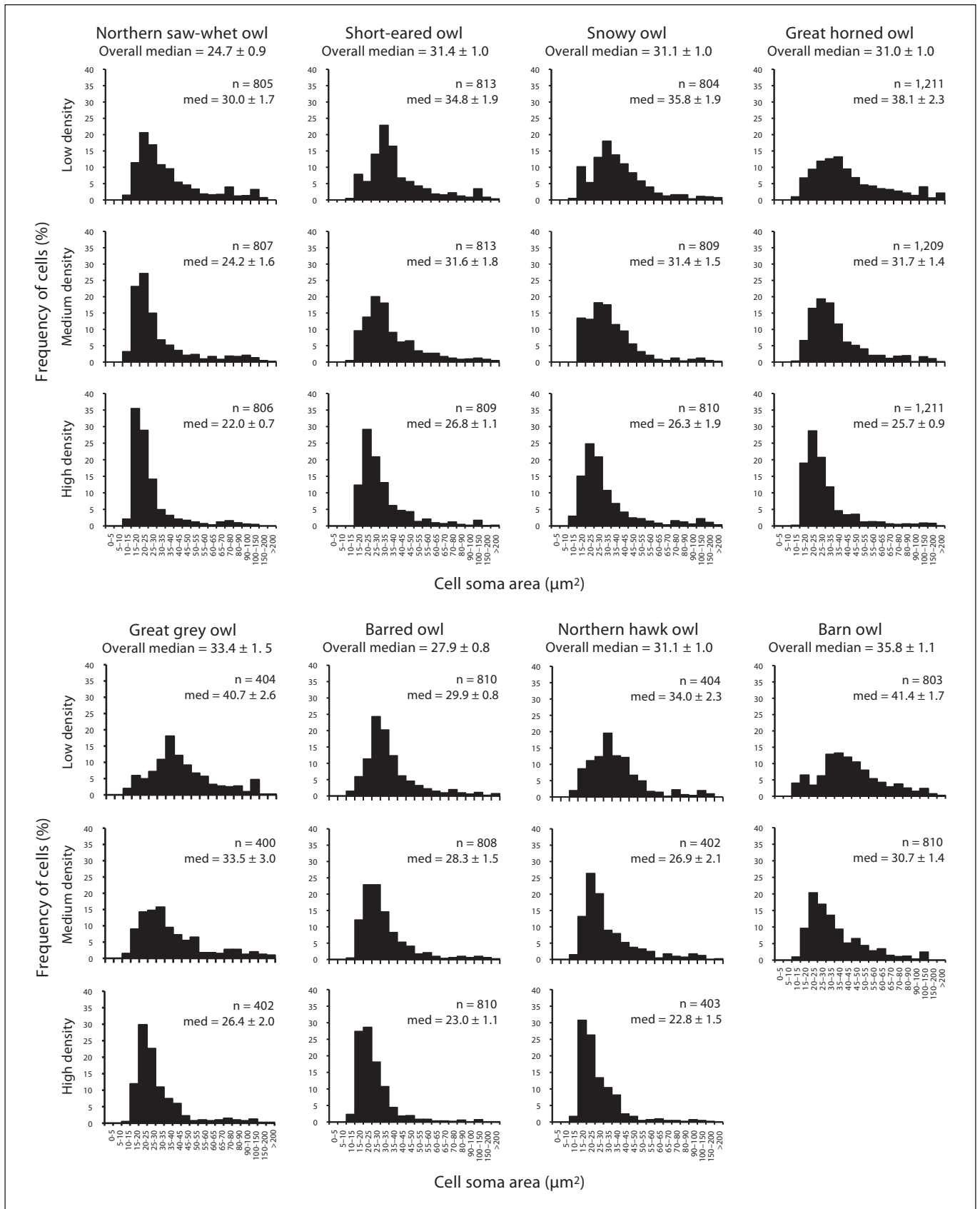
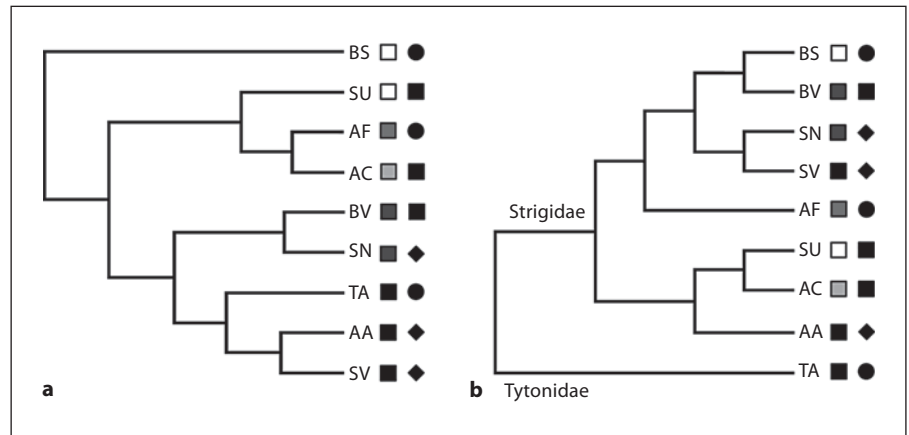


Fig. 7. **a** Hierarchical cluster analysis dendrogram based on eye shape and three retinal topography variables (peak cell density, centrop peripheral density gradient and H:V ratio) for nine species of owl. **b** Phylogenetic tree showing the relationships between the same nine species [based on Wink et al., 2008]. Following table 1, the species names are abbreviated and the shading of the symbols reflects the activity pattern and habitat preference of each owl species.



to that which we could obtain from wildlife sanctuaries, veterinary clinics and donations from other researchers. While sanctuaries and veterinarians represent important sources of material for comparative studies such as this, it should be noted that a high proportion of the owls they receive exhibit eye trauma [Cousquer, 2005; Williams et al., 2006; Seruca et al., 2011]. Therefore, we were not able to account for individual variation in some of the owl species we investigated. However, for the few species for which multiple eyes were available, eye shape, retinal topography and H:V ratio were consistent between individuals. Also, our results for the barn owl are consistent with the findings of Wathey and Pettigrew [1989]. Eye shape/ocular dimensions and retinal topography are generally considered to be highly species-specific characteristics in vertebrates [Hughes, 1977; Martin, 1982; Collin, 1999, 2008; Howland et al., 2004]. This is emphasized, for example, by the convention of presenting only one representative retinal topography map for a given species. Only rarely are multiple maps for the same species presented in the same publication, and in these the retinal topography is consistent across individuals of the same age or size class [Boire et al., 2001; Pettigrew et al., 2010]. Studies that have analyzed multiple eyes from the same species have also consistently reported minimal variation in eye shape and retinal topography among individuals [Binggeli and Paule, 1969; Ehrlich, 1981; Collin and Pettigrew, 1988b, c; Schaeffel and Howland, 1988; Boire et al., 2001; Lisney and Collin, 2008; Dolan and Fernández-Juricic, 2010; Fernández-Juricic et al., 2011]. Therefore, we are confident that the results presented here represent real interspecific variation in eye shape and retinal topography in owls and are unlikely to be affected by intraspecific variation.

Eye Shape and Activity Pattern

Consistent patterns of variation in eye shape in relation to activity patterns and habitats have been reported across vertebrates [Walls, 1942; Hughes, 1977; Kirk, 2004; Warrant, 2004; Ross et al., 2007; Hall, 2008; Schmitz and Wainwright, 2011], including birds [Martin, 1994; Hall and Ross, 2007; Iwaniuk et al., 2010a; Corfield et al., 2011]. For example, across a diverse sample of over 450 bird species, Hall and Ross [2007] have recently shown that there are significant differences in eye shape among birds with nocturnal, crepuscular/cathemeral and diurnal activity patterns. Nocturnal birds have higher CD:AL ratios compared to diurnal birds, while crepuscular/cathemeral species have intermediate CD:AL ratios. These differences reflect differences in the light-gathering capabilities of eyes that operate under luminance levels that vary by about 12 log units [Martin, 1982; Land and Nilsson, 2002; Warrant, 2004]. Within the owls that we sampled, we observed the same general overall pattern (fig. 1, 2). Nocturnal species have the highest CD:AL ratios and diurnal owls have the lowest, with species active during crepuscular time periods having intermediate CD:AL ratios. Furthermore, the average CD:AL ratios for the nocturnal (-0.149) and diurnal (-0.223) owls from our study are very similar to those across all birds presented by Hall and Ross [2007].

The CD:AL ratios for the burrowing and short-eared owls are more similar to those of nocturnal and nocturnal/crepuscular owls, despite the fact that we classified the species as being diurnal/crepuscular and crepuscular/cathemeral, respectively, on the basis of the consensus of the literature (table 1). Thus, the eye shape data suggest that these species are more concerned with increasing retinal illumination than may have been expected given their

reported ecological niches. Despite the activity pattern classifications we have assigned to these owls, both species have been reported to exhibit a preference for hunting under low light intensities [Clark, 1975; Haug and Oliphant, 1990; Reynolds and Gorman, 1999]. As field studies of owl behavior based on observations can be biased towards crepuscular and daylight hours when the owls are visible to human observers [Haug and Oliphant, 1990; Calladine et al., 2010], more radiotelemetry studies will be important to better define the activity patterns of these species.

Retinal Topography and Activity Pattern and Habitat

Relationships between retinal topography and the perceived openness of the perceived world of a species are well documented [Hughes, 1977; Collin, 1999, 2008]. A visual streak is commonly associated with diurnal vertebrates that live in open habitats. This retinal specialization is proposed to allow species to view the horizon, over which new visual targets are most likely to appear, with increased spatial resolving power and without the need for extensive eye or head movements. It has also been suggested that visual streaks may be important for orientating the eye with respect to the horizon [Meyer, 1977]. Alternatively, in nocturnal vertebrates or vertebrates that live in architecturally complex enclosed habitats, the cells in the RGC layer tend to be arranged in a more radially symmetrical pattern [Hughes, 1977; Collin, 1999]. As opposed to species with well-defined visual streaks, such species generally rely more on eye/head movements to fixate these areas of high cell density onto visual targets of interest [Collin, 1999, 2008]. These relationships have been previously demonstrated in birds. For example, a number of diurnal birds from open habitats have visual streaks, including Procellariiform seabirds [Hayes and Brooke, 1990; Hayes et al., 1991], the ostrich [*Struthio camelus*; Boire et al., 2001] and the Canada goose [*Branta canadensis*; Fernández-Juricic et al., 2011], while a variety of woodland species [Moroney and Pettigrew, 1987; Dolan and Fernández-Juricic, 2010] and the Kerguelen petrel (*Lugensa brevirostris*), a nocturnal Procellariiform seabird [Hayes and Brooke, 1990], have a more radially symmetrical retinal topography. In this study, we provide evidence that the terrain theory of Hughes [1977] also applies within an avian order (Strigiformes), thus building upon previous works on owls [Bravo and Pettigrew, 1981; Wathey and Pettigrew, 1989].

The species with the most well-defined visual streak and the highest H:V ratio (3.88), the snowy owl, is diurnally active in open habitats such as tundra or snow-covered grassland [Boxall and Lein, 1982; del Hoyo et al.,

1999; König and Weick, 2008]. Well-defined visual streaks with lower H:V ratios ranging from 2.92 to 2.33 were found in four other owl species that prefer open or mixed habits, the short-eared, northern hawk, burrowing and great horned owls, although these species exhibit a range of activity patterns, from diurnal (northern hawk owl) to nocturnal/crepuscular (great horned owl) (table 1). The visual streaks in these owls may be particularly useful for surveying open country for prey, especially in species that hunt from perches (the burrowing, great horned, snowy, and northern hawk owls) [Jaksić and Carothers, 1985; Sonnerud, 1992; del Hoyo et al., 1999; König and Weick, 2008]. For species that spend a significant amount of time on the ground (such as the short-eared, burrowing and snowy owls) the visual streak may play an important role in predator detection [Wiklund and Stigh, 1983; Voous, 1988; König and Weick, 2008].

The owls that display poorly defined visual streaks with H:V ratios >2 (the northern saw-whet, barred, great grey and barn owls) are nocturnal or nocturnal/crepuscular species and, with the exception of the barn owl, live in forest habitats (table 1). For these owls, the visual horizon is at least partially obscured by vegetation and/or darkness and so presumably does not represent a major component of the perceived worlds of these species. The northern saw-whet, barred, great grey and barn owls have some degree of ear asymmetry and auditory nuclei enlargement, suggesting that they might rely more upon auditory cues than other owls [Norberg, 1977; Gutiérrez-Ibáñez et al., 2011]. For example, barn owls and great grey owls are capable of capturing prey in the total absence of visual cues [Nero, 1980; Takahashi, 2010]. Thus, the low H:V ratios in these species could reflect, at least in part, a decreased reliance on visual cues compared to the species with much higher H:V ratios such as the snowy owl.

Presence of a Fovea

All of the owl species we examined had an area of high cell density located in the temporal retina. In seven of the eight strigid owls, a fovea was positively identified in the high density area. Our estimates of peak cell densities for the strigid owls we investigated (22,335–34,157 cells mm^{-2}) are in keeping with peak densities reported previously for owls from this family [Fite and Rosenfield-Wessels, 1975; Bravo and Pettigrew, 1981]. No fovea was found in the tytonid barn owl and the area centralis in this species had a lower average peak cell density (16,780 cells mm^{-2}) than those of the strigid owls, which is consistent with previous findings [Oehme, 1961; Bravo and Pettigrew, 1981; Wathey and Pettigrew, 1989]. Our inability to

identify a fovea in the great grey owl does not, however, necessarily mean that this species lacks a fovea. It is not uncommon for the foveal regions of a retina to be torn during the wholemounting and drying process [Bravo and Pettigrew, 1981], and unfortunately only one eye from this species was available to us because the other eye was damaged by trauma. However, a fovea has been described in all other strigid owl species previously investigated [Wood, 1917; Rochon-Duvigneaud, 1943; Oehme, 1961; Fite, 1973; Bravo and Pettigrew, 1981] including two other *Strix* species, the tawny owl *Strix aluco* [Oehme, 1961] and the barred owl (this study). We therefore think it is likely that the great grey owl also possesses a fovea.

Influence of Amacrine Cells in the RGC Layer

In birds, estimates of the number of 'displaced' amacrine cells in the RGC layer have been made using various methods. These include comparing the total number of cells in the RGC layer with the total number of fibers in the optic nerve [Binggeli and Paule, 1969; Wathey and Pettigrew, 1989], cell degeneration following retina lesions or optic nerve axotomy [Ehrlich, 1981; Chen and Naito, 1999], retrograde labeling [Chen and Naito, 1999] or identifying amacrine cells using cytological properties [Hart, 2002; Coimbra et al., 2006]. In birds, the proportion of cells in the RGC layer accounted for by the displaced amacrine cell population ranges, for example, from 15 to 19% in tyrant flycatchers [Coimbra et al., 2006], from 11 to 43% in the pigeon [Binggeli and Paule, 1969; Hayes, 1984], from 30 to 35% in the chick [Ehrlich, 1981; Chen and Naito, 1999] and 50% in the barn owl [Wathey and Pettigrew, 1989]. Given that we have included the displaced amacrine cell population in our counts, the RGC numbers and densities calculated for owls in this study are clearly overestimates. However, as discussed previously, for vertebrates (including owls) for whom RGC topography has been assessed using both Nissl staining and retrograde labeling, both the peak cell densities and the overall topographic distribution of cells remain relatively similar despite the inclusion of the displaced amacrine cells [Bravo and Pettigrew, 1981; Collin, 1988, 1999; Collin and Pettigrew, 1988; Pettigrew et al., 1988; Chen and Naito, 1999]. Thus, we are confident that the inclusion of the displaced amacrine cell population in our results does not unduly influence the overall retinal topography in any of the owls assessed.

Cell Size-Frequency Distributions

Median cell soma area is inversely proportional to cell density in owls and increases towards the retinal periph-

ery. The cells in the more central, higher-density retinal regions of the retina form a more homogeneous population compared to those in the peripheral, low-density parts of the retina. This mirrors the situation in other birds [Ehrlich, 1981; Hayes and Brooke, 1990; Inzunza et al., 1991; Chen and Naito, 1999; Boire et al., 2001; Dolan and Fernández-Juricic, 2010] and vertebrates in general [Tancred, 1981; Frank and Hollyfield, 1987; Collin, 1988; Collin and Pettigrew, 1988; Silveira et al., 1989; Bailes et al., 2006; Lisney and Collin, 2008].

Our results indicate that a range of RGC size classes are present in owls. This is consistent with the study of Bravo and Pettigrew [1981], which identified retrograde-labeled RGCs with soma sizes ranging from 20 to 1,200 μm^2 in the burrowing and barn owls. This in turn suggests that a number of different RGC classes are represented in the retinas of owls, which may have different functional properties [Saito, 1983]. Bravo and Pettigrew [1981] classified the RGCs in owls into four groups based on soma size (small, medium, large and very large). Using more sophisticated intracellular filling and retrograde-labeling techniques, however, Naito and Chen [2004] identified 6 major RGC types and 26 subtypes in the chick on the basis of RGC soma size and the field size, arborization and stratification in the inner plexiform layer of the dendrites. Therefore, more detailed study will be required to identify specific morphological RGC subtypes in owls and to note whether the number or distribution of these cells varies among species.

Small numbers of very large RGCs were identified in all of the owl species examined. These cells have similar characteristics (soma areas $>150 \mu\text{m}^2$ and 2–4 primary dendrites) to the 'giant ganglion cells' identified in other nonmammalian vertebrates [Stell and Witkovsky, 1973; Collin and Northcutt, 1993] including birds [Bravo and Pettigrew, 1981; Hayes et al., 1991; Coimbra et al., 2006, 2009]. The cells appear comparable to the alpha RGCs in mammals, which mediate motion sensitivity [Peichl, 1991]. The specific distribution of these cells has been mapped in some avian species, resulting in the identification of a specialized area of high giant RGC density termed an 'area gigante cellularis' in the temporal retina, which is thought to be involved in behaviors that require movement detection [Hayes et al., 1991; Coimbra et al., 2006, 2009]. Topographic mapping of the large RGC population in owls was not undertaken here, but preliminary analyses of the great horned owl indicate that although large RGCs are sparsely distributed across the retina, the highest densities are found temporal to the fovea [Lisney T, unpubl. data].

Retinotectal Projections

In the study of Bravo and Pettigrew [1981] on the barn owl and the burrowing owl, retrograde labeling revealed that a relatively homogenous population of RGCs (in terms of soma size) in the temporal part of the retina, including the area centralis or fovea, projects contralaterally to the thalamus, while a far more heterogeneous population of RGCs in the visual streak projects contralaterally to the optic tectum. Moreover, in the barn owl a higher proportion of the total RGC population projects to the tectum as opposed to the thalamus compared to the burrowing owl. Given the differences in the organization of the visual streak between these two species [Bravo and Pettigrew, 1981; Wathey and Pettigrew, 1989] and other owls, it is plausible that differences in retinal topography may be reflected centrally in the organization of the optic tectum [Peterson, 1981]. There is some evidence that tectum volume scales very closely with total brain volume in owls [Iwaniuk et al., 2010b]; for example, data on tectum volume from similarly sized barn owl and burrowing owl brains (with volumes of 6,149 and 5,878 mm⁻³, respectively) indicate that the tectum accounts for a very similar proportion of the brain in both species (2.22 and 2.53%, respectively). Insufficient information exists at present to speculate any further but a detailed comparative investigation of the retinorecipient brain areas in owls is under way [Gutiérrez-Ibáñez C, Iwaniuk AN, Lisney TJ and Wylie DR, unpubl. data].

Evolution of Owl Visual Systems

Our results provide evidence of interspecific variation in eye shape and retinal topography in owls. This variation is associated with different activity patterns and habitat preferences as opposed to phylogenetic relationships between species as reflected by the clustering of species on the basis of similarities in eye shape and retinal topography (fig. 7). These results support the findings of previous studies on retinal organization [Oehme, 1961; Bravo and Pettigrew, 1981] and physiological optics [Murphy and Howland, 1983; Howland et al., 1991] and indicate that the organization of the visual systems of these birds can be quite varied and closely associated with the ecological niches of different species. Therefore, some caution should be employed when using owls as representative nocturnal birds in comparisons with other species.

It is not clear whether the interspecific variation seen in owl visual systems represents preadaptations that then allow different species to be successful in new ecological niches, or whether they represent adaptations to the selection pressures imposed by their present ecological niches. Over the course of owl evolution there appear to have been

a number of independent transitions from a nocturnal to a more crepuscular or diurnal lifestyle [del Hoyo et al., 1999; König and Weick, 2008]. For example, while members of the genera *Aegolius*, *Otus*, *Phodilus*, *Strix* and *Tyto* are generally considered to be nocturnal or nocturnal/crepuscular, variation in activity pattern has been reported within *Asio* and *Bubo* and most members of the genera *Athene*, *Glaucidium* and *Surnia* are considered to be largely crepuscular or diurnal. Similarly, while most owls live in woodland or forest habitats, a number of genera contain species that inhabit more open habitats (e.g. *Asio*, *Athene*, *Bubo*, *Glaucidium*, *Tyto*) [del Hoyo et al., 1999; König and Weick, 2008]. Therefore, a more detailed analysis using phylogenetic comparative methods, performed on more owl genera, and potentially using more visual system variables (e.g. rod:cone ratios, photoreceptor dimensions) will be necessary to address this issue.

The one tytonid owl we examined, the barn owl, showed marked differences from the strigid owls that we examined with respect to its retinal morphology, i.e. relatively low numbers of large cells in the RGC layer and the lack of a fovea. It will therefore be important to assess the eyes of other tytonid owls in order to confirm whether this is true of all tytonid owls. One aspect of the tytonid visual system worth mentioning in this context is a study of accommodation among tytonid owls [Howland et al., 1991]. The North American barn owl (*T. alba pratincola*) had a greater accommodative range than three other *Tyto* species, which likely reflects species variation in activity pattern and diet [Howland et al., 1991]. Given this behavioral variation within the genus *Tyto*, there may be anatomical differences in the visual system within *Tyto* as well as *Phodilus* (bay owls), the other genus within the Tytonidae.

In summary, our data suggest that both activity pattern and habitat can play an important role in the evolution of eye shape and retinal topography in owls. Given that birds in general occupy a wide range of habitats and ecological niches and that evolutionary changes in activity pattern have occurred throughout avian evolution, further studies are required to determine the extent to which our results can be applied to other avian orders, especially those orders with species that vary in activity pattern, e.g. Charadriiformes [Iwaniuk et al. 2010a].

Acknowledgments

We would like to thank the Alberta Institute for Wildlife Conservation and Catherine Carr (University of Maryland) for providing us with specimens for this study and Cristian Gutiérrez-Ibáñez and David Graham for useful discussions and logistical support.

References

- Bailes HJ, Trezise AEO, Collin SP (2006): The number, morphology, and distribution of retinal ganglion cells and optic axons in the Australian lungfish *Neoceratodus forsteri* (Krefft 1870). *Vis Neurosci* 23:257–272.
- Binggeli RL, Paule WJ (1969): The pigeon retina: quantitative aspects of optic nerve and ganglion cell layer. *J Comp Neurol* 137:1–18.
- Boire D, Dufour JS, Theoret H, Ptito M (2001): Quantitative analysis of the retinal ganglion cell layer in the ostrich, *Struthio camelus*. *Brain Behav Evol* 58:343–355.
- Boxall PC, Lein MR (1982): Feeding ecology of snowy owls (*Nyctea scandiaca*) wintering in southern Alberta. *Arctic* 35:282–290.
- Braekvelt CR (1993): Fine structure of the retinal photoreceptors of the great horned owl (*Bubo virginianus*). *Histol Histopathol* 8:25–34.
- Braekvelt CR, Smith SA, Smith BJ (1996): Fine structure of the retinal photoreceptors of the barred owl (*Strix varia*). *Histol Histopathol* 11:79–88.
- Bravo H, Pettigrew JD (1981): The distribution of neurons projecting from the retina and visual cortex to the thalamus and tectum opticum of the barn owl, *Tyto alba*, and burrowing owl, *Speotyto cunicularia*. *J Comp Neurol* 199:419–441.
- Calladine J, Garner G, Wernham C, Buxton N (2010): Variation in the diurnal activity of breeding short-eared owl *Asio flammeus*: implications for their survey and monitoring. *Bird Study* 57:89–99.
- Chen Y, Naito J (1999): A quantitative analysis of the cells in the ganglion cell layer of the chick retina. *Brain Behav Evol* 53:75–86.
- Clark RJ (1975): A field study of the short-eared owl, *Asio flammeus* (Pontoppidan), in North America. *Wildl Monogr* 47:1–67.
- Coimbra JP, Marceliano MLV, Andrade-da-Costa BLS, Yamada ES (2006): The retina of tyrant flycatchers: topographic organization of neuronal density and size in the ganglion cell layer of the great kiskadee *Pitangus sulphuratus* and the rusty margined flycatcher *Myiozetetes cayanensis* (Aves: Tyrannidae). *Brain Behav Evol* 68:15–25.
- Coimbra JP, Trévia N, Marceliano ML, da Silveira Andrade-Da-Costa BL, Picanço-Diniz CW, Yamada ES (2009): Number and distribution of neurons in the retinal ganglion cell layer in relation to foraging behaviors of tyrant flycatchers. *J Comp Neurol* 514:66–73.
- Collin SP (1988) the retina of the shovel-nosed ray, *Rhinobatos batillum* (Rhinobatidae): morphology and quantitative analysis of the ganglion, amacrine and bipolar cell populations. *Exp Biol* 47:195–207.
- Collin SP (1999): Behavioural ecology and retinal cell topography; in Archer SN, Djamgoz MBS, Loew ER, Partridge JC, Vellarga S (eds): *Adaptive Mechanisms in the Ecology of Vision*. Dordrecht, Kluwer Academic Publishers, pp 509–535.
- Collin SP (2008): A web-based archive for topographic maps of retinal cell distribution in vertebrates. *Clin Exp Optom* 91:85–95.
- Collin SP, Northcutt RG (1993): The visual system of the Florida garfish, *Lepisosteus platyrhinchus* (Ginglymodi). III. Retinal ganglion cells. *Brain Behav Evol* 42:295–320.
- Collin SP, Partridge JC (1996): Retinal specializations in the eyes of deep-sea teleosts. *J Fish Biol* 49(suppl A):157–174.
- Collin SP, Pettigrew JD (1988a): Retinal ganglion cell topography in teleosts: a comparison between Nissl-stained material and retrograde labelling from the optic nerve. *J Comp Neurol* 276:412–422.
- Collin SP, Pettigrew JD (1988b): Retinal topography in reef teleosts. I. Some species with well-developed areas but poorly-developed streaks. *Brain Behav Evol* 31:269–282.
- Collin SP, Pettigrew JD (1988c): Retinal topography in reef teleosts. II. Some species with prominent horizontal streaks and high-density areas. *Brain Behav Evol* 31:283–295.
- Corfield JR, Gsell AC, Brunton D, Heesy CP, Hall MI, Acosta ML, Iwaniuk AI (2011): Anatomical specializations for nocturnality in a critically endangered parrot, the kakapo (*Strigops habroptilus*). *PLoS ONE* 6:e22945.
- Cousquer G (2005): Ophthalmological findings in free-living tawny owls (*Strix aluco*) examined at a wildlife veterinary hospital. *Vet Rec* 156:734–739.
- del Hoyo J, Elliott A, Sargatal J (eds) (1999): *Handbook of the Birds of the World*, vol 5: *Barn-Owls to Hummingbirds*. Barcelona, Lynx Edicions.
- Dolan T, Fernández-Juricic E (2010): Retinal ganglion cell topography of five species of ground-foraging birds. *Brain Behav Evol* 75:111–121.
- Duncan JR (1997): Great grey owls (*Strix nebulosa nebulosa*) and forest management in North America: a review and recommendations. *J Raptor Res* 31:160–166.
- Duncan JR, Harris WC (1997): Northern hawk owls (*Surnia ulula caparoch*) and forest management in North America: a review. *J Raptor Res* 31:187–190.
- Ehrlich D (1981): Regional specialization of the chick retina as revealed by the size and density of neurons in the ganglion cell layer. *J Comp Neurol* 195:643–657.
- Fast SJ, Ambrose HW III (1976): Prey preference and hunting habitat selection in the barn owl. *Am Midl Nat* 96:503–507.
- Fernández-Juricic E, Moore BA, Doppler M, Freeman J, Blackwell BF, Lima SL, DeVault TL (2011): Testing the terrain hypothesis: Canada geese see their world laterally and obliquely. *Brain Behav Evol* 77:147–158.
- Fischer QS, Kirby MA (1991): Number and distribution of retinal ganglion cells in anubis baboons (*Papio Anubis*). *Brain Behav Evol* 37:189–203.
- Fite KV (1973): Anatomical and behavioral correlates of visual acuity in the great horned owl. *Vision Res* 13:219–230.
- Fite KV, Rosenfield-Wessels S (1975): A comparative study of deep avian foveas. *Brain Behav Evol* 12:97–115.
- Forbes JE, Warner DW (1974): Behavior of a radio-tagged saw-whet owl. *Auk* 91:783–795.
- Frank BD, Hollyfield JG (1987): Retinal ganglion cell morphology in the frog, *Rana pipiens*. *J Comp Neurol* 266:413–434.
- Glaser EM, Wilson PD (1998): The coefficient of error of optical fractionator population size estimates: a computer simulation comparing three estimators. *J Microsc* 192:163–171.
- Gundersen HJG (1977): Notes on the estimation of the numerical density of arbitrary particles: the edge effect. *J Microsc* 111:219–223.
- Gutiérrez-Ibáñez C, Iwaniuk AN, Wylie DR (2011): Relative size of auditory pathways in symmetrically and asymmetrically eared owls. *Brain Behav Evol* 87:286–301.
- Hall MI (2008): Comparative analysis of the size and shape of the lizard eye. *Zoology* 111:62–75.
- Hall MI, Heesy CP (2010): Eye size, flight speed and Leuckart's Law in birds. *J Zool* 283:291–297.
- Hall MI, Ross CF (2007): Eye shape and activity pattern in birds. *J Zool* 271:437–444.
- Hammer Ø, Harper DAT, Ryan PD (2001): *PAST: Palaeontological Statistics Software Package for Education and Data Analysis*. *Palaeontol Electron* 4:1–9.
- Harmening WM, Wagner H (2011): From optics to attention: visual perception in barn owls. *J Comp Physiol A* 197:1031–1042.
- Hart NS (2001): Variation in cone photoreceptor abundance and the visual ecology of birds. *J Comp Physiol A* 187:685–698.
- Hart NS (2002): Vision in the peafowl (Aves: *Pavo cristatus*). *J Exp Biol* 205:3925–3935.
- Haug EA, Oliphant LW (1990): Movements, activity patterns, and habitat use of burrowing owls in Saskatchewan. *J Wildl Manage* 54:27–35.
- Hayes BP (1984): Cell populations of the ganglion cell layer: displaced amacrine and matching cells in the pigeon retina. *Exp Brain Res* 56:565–573.
- Hayes BP, Brooke MD (1990): Retinal ganglion cell distribution and behavior in Procellariiform seabirds. *Vision Res* 30:1277–1289.
- Hayes B, Martin GR, Brooke M de L. (1991): Novel area serving binocular vision in the retinae of procellariiform seabirds. *Brain Behav Evol* 37:79–84.
- Hayward GD, Garton EO (1988): Resource partitioning among forest owls in the River of No Return Wilderness, Idaho. *Oecologia* 75:253–265.
- Hocking B, Mitchell BL (1961): Owl vision. *Ibis* 103a:284–288.

- Howard CV, Reed MG (2005): Unbiased Stereology: Three-Dimensional Measurement in Microscopy, ed 2. Abingdon, BIOS Scientific Publishers.
- Howland HC, Howland MJ, Schmid K, Pettigrew JD (1991): Restricted range of ocular accommodation in barn owls (Aves: Tytonidae). *J Comp Physiol A* 168:299–303.
- Howland HC, Merola S, Basarab JR (2004): The allometry and scaling of the size of vertebrate eyes. *Vision Res* 44:2043–2065.
- Hughes A (1977): The topography of vision in mammals of contrasting lifestyles: comparative optics and retinal organization; in Cresitelli F (ed): *Handbook of Sensory Physiology*, vol VIII/5. Berlin, Springer, pp 613–756.
- Hughes A (1985): New perspectives in retinal organization; in Osbourne NN, Chader G, (eds): *Progress in Retinal Research*. New York, Pergamon Press, pp 243–313.
- Inzunza O, Bravo H, Smith RL, Angel M (1991): Topography and morphology of retinal ganglion cells in Falconiforms: a study on predatory and carrion-eating birds. *Anat Rec* 229: 271–277.
- Iwaniuk AN, Gutiérrez-Ibáñez C, Pakan JMP, Wylie DR (2010b): Allometric scaling of the tectofugal pathway in birds. *Brain Behav Evol* 75:122–137.
- Iwaniuk AN, Heesy CP, Hall MI (2010a): Morphometrics of the eyes and orbits of the nocturnal swallow-tailed gull (*Creagrurus furcatus*). *Can J Zool* 88:855–865.
- Iwaniuk AN, Hurd PL (2005): The evolution of cerebrotypes in birds. *Brain Behav Evol* 65: 215–230.
- Iwaniuk AN, Hurd PL, Wylie DRW (2006): The comparative morphology of the cerebellum in caprimulgidiform birds: evolutionary and functional implications. *Brain Behav Evol* 67:53–68.
- Jaksić FM, Carothers JH (1985): Ecological, morphological, and bioenergetic correlates of hunting mode in hawks and owls. *Ornis Scand* 16:165–172.
- Kirk EC (2004): Comparative morphology of the eye in primates. *Anat Rec* 281A:1095–1103.
- König C, Weick F (2008): *Owls of the World*, ed 2. London, Christopher Helm.
- Land MF, Nilsson DE (2002): *Animal Eyes*. Oxford, Oxford University Press.
- Lisney TJ, Collin SP (2008): Retinal ganglion cell distribution and spatial resolving power in elasmobranchs. *Brain Behav Evol* 72:59–77.
- Lisney TJ, Rubene D, Rózsa J, Løvlie H, Håstad O, Ödeen A (2011): Behavioural assessment of flicker fusion frequency in chicken *Gallus gallus domesticus*. *Vision Res* 51:1324–1332.
- Lythgoe JN (1979): *The Ecology of Vision*. Oxford, Oxford University Press.
- Marti MD (1974): Feeding ecology of four sympatric owls. *Condor* 76:45–61.
- Martin GR (1977): Absolute visual threshold and scotopic spectral sensitivity in the tawny owl *Strix aluco*. *Nature* 268:636–638.
- Martin GR (1982): An owl's eye: schematic optics and visual performance in *Strix aluco* L. *J Comp Physiol A* 145:341–349.
- Martin GR (1986): Sensory capacities and the nocturnal habit of owls (Strigiformes). *Ibis* 128:266–277.
- Martin GR (1994): Form and function in the optical structure of bird eyes; in Davies MNO, Green PR (eds): *Perception and Motor Control in Birds. An Ecological Approach*. Berlin, Springer, pp 5–34.
- Martin GR, Gordon IE (1974): Visual acuity in the tawny owl (*Strix aluco*). *Vision Res* 14: 1393–1397.
- Mazur KM (1997): Spatial Habitat Selection by Barred Owls (*Strix varia*) in the Boreal Forest of Saskatchewan, Canada; MS thesis, University of Regina, Regina.
- Meyer DB (1977): The avian eye and its adaptations; in Cresitelli F (ed): *Handbook of Sensory Physiology*, vol VIII/5. Berlin, Springer, pp 549–611.
- Mooi E, Sarstedt M (2011): *A Concise Guide to Market Research*. Berlin, Springer.
- Moroney MK, Pettigrew JD (1987): Some observations on the visual optics of kingfishers (Aves, Coraciiformes, Alcedinidae). *J Comp Physiol A* 160:137–149.
- Murphy CJ, Howland HC (1983): Owl eyes: accommodation, corneal curvature and refractive state. *J Comp Physiol A* 151:277–284.
- Naito J, Chen Y (2004): Morphologic analysis and classification of ganglion cells of the chick retina by intracellular injection of lucifer yellow and retrograde labeling with DiI. *J Comp Neurol* 469:360–376.
- Nero RW (1980): *The Great Gray Owl – Phantom of the Northern Forest*. Washington, Smithsonian Institution Press.
- New STD, Bull CM (2011): Retinal ganglion cell topography and visual acuity of the sleepy lizard (*Tiliqua rugosa*). *J Comp Physiol A* 197:703–709.
- Nicholls TH, Warner DW (1972): Barred owls habitat use as determined by radiotelemetry. *J Wildl Manage* 36:213–224.
- Norberg RA (1977): Occurrence and independent evolution of bilateral ear asymmetry in owls and implications on owl taxonomy. *Philos Trans R Soc Lond B* 280:375–408.
- Oehme H (1961): Vergleichend-histologische Untersuchungen an der Retina von Eulen. *Zool Jahrb Anat* 79:439–478.
- Oehme H (1962): Das Auge von Mauersegler, Star und Amsel. *J Ornithol* 103:187–212.
- Partridge JC (1989): The visual ecology of avian cone oil droplets. *J Comp Physiol A* 165:415–426.
- Peichl L (1991): Alpha ganglion cells in mammalian retinae: common properties, species differences, and some comments on other ganglion cells. *Vis Neurosci* 7:155–169.
- Peterson EH (1981): Regional specialization in retinal ganglion cell projection to optic tectum of *Dipsosaurus dorsalis* (Iguanidae). *J Comp Neurol* 196:225–252.
- Pettigrew JD, Bhagwandin A, Haagensen M, Manger PR (2010): Visual acuity and heterogeneities of retinal ganglion cell densities and the tapetum lucidum of the African elephant (*Loxodonta africana*). *Brain Behav Evol* 75:251–261.
- Pettigrew JD, Dreher B, Hopkins CS, McCall MJ, Brown M (1988): Peak density and distribution of ganglion cells in the retinae of microchiropteran bats: implications for visual acuity. *Brain Behav Evol* 32:39–56.
- Pettigrew JD, Manger PR (2008): Retinal ganglion cell density of the black rhinoceros (*Diceros bicornis*): calculating visual resolution. *Vis Neurosci* 25:215–220.
- Quinn GP, Keough MJ (2002): *Experimental Design and Data Analysis for Biologists*. Cambridge, University of Cambridge Press.
- Rasband WS (1997–2011): *Image J*. Bethesda, US National Institutes of Health.
- Rehkaemper G, Kart E, Frahm HD, Werner CW (2003): Discontinuous variability of brain composition among domestic chicken breeds. *Brain Behav Evol* 61:59–69.
- Reynolds P, Gorman ML (1999): The timing of hunting in short-eared owls (*Asio flammeus*) in relation to the activity patterns of Orkney voles (*Microtus arvalis orcadensis*). *J Zool* 247:371–379.
- Ritland S (1982): *The Allometry of the Vertebrate Eye*; PhD thesis, University of Chicago, Chicago.
- Rochon-Duvigneaud A (1943): *Les Yeux et le Vision des Vertèbres*. Paris, Masson.
- Ross CF, Hall MI, Heesy CP (2007): Were basal primates nocturnal? Evidence from eye and orbit shape; in Ravosa MJ, Dagosto M (eds): *Primate Origins: Adaptations and Evolution*. New York, Springer, pp 223–256.
- Rudolph SG (1978): Predation ecology of coexisting great horned and barn owls. *Wilson Bull* 90:134–137.
- Saito H-A (1983): Morphology of physiologically identified X-, Y-, and W-type retinal ganglions of the cat. *J Comp Neurol* 221:279–288.
- Schaeffel F, Howland HC (1988): Visual optics in normal and ametropic chickens. *Clin Vision Sci* 3:83–98.
- Schaeffer RL, Mendenhall W, Ott L (1996): *Elementary Survey Sampling*, ed 5. Boston, PWS-Kent.
- Schmitz L, Wainwright PC (2011): Nocturnality constrains morphological and functional diversity in the eyes of reef fishes. *BMC Evol Biol* 11:338.
- Seruca C, Molina-López R, Peña T, Leiva M (2011): Ocular consequences of blunt trauma in two species of nocturnal raptors (*Athene noctua* and *Otus scops*). *Vet Ophthalmol*, Epub ahead of print.

- Silveira LCL, Diniz-Picanco CW, Oswaldo-Cruz E (1989): Distribution and size of ganglion cells in the retinae of large Amazon rodents. *Vis Neurosci* 2:221–235.
- Sonerud GA (1992): Search tactics of a pause-travel predator: adaptive adjustments of perching times and move distances by hawk owls (*Surnia ulula*). *Behav Ecol Sociobiol* 30: 207–217.
- Stell WK, Witkovsky P (1973): Retinal structure in the smooth dogfish *Mustelus canis*: general description and light microscopy of giant ganglion cells. *J Comp Neurol* 148:1–32.
- Stone J (1981): *The Wholemound Handbook: A Guide to the Preparation and Analysis of Retinal Wholemounds*. Sydney, Clarendon Press.
- Stone J, Keens J (1980): Distribution of small and medium-sized ganglion cells in the cat's retina. *J Comp Neurol* 192:235–246.
- Takahashi TT (2010): How the owl tracks its prey – II. *J Exp Biol* 213:3399–3408.
- Tancred E (1981): The distribution and sizes of ganglion cells in the retinas of five Australian marsupials. *J Comp Neurol* 196:585–603.
- Tester JR (1987): Changes in daily activity rhythms of some free-ranging animals in Minnesota. *Can Field Nat* 101:13–21.
- Ullmann JFP, Moore BA, Temple SH, Fernández-Juricic E, Collin SP (2012): The retinal wholemound technique: a window to understanding the brain and behaviour. *Brain Behav Evol* 79:26–44.
- Vaney DI (1980): A quantitative comparison between the ganglion cell populations and axonal outflows of the visual streak and periphery of the rabbit retina. *J Comp Neurol* 189: 215–233.
- Voous KH (1988): *Owls of the Northern Hemisphere*. Cambridge, MIT Press.
- Walls GL (1942): *The Vertebrate Eye and Its Adaptive Radiation*. Bloomfield Hills, Cranbrook Institute of Science.
- Warrant E (2004): Vision in the dimmest habitats on Earth. *J Comp Physiol A* 190:765–789.
- Wathey JC, Pettigrew JD (1989): Quantitative analysis of the retinal ganglion cell layer and optic nerve of the barn owl *Tyto alba*. *Brain Behav Evol* 33:279–292.
- Wiklund CG, Stigh J (1983): Nest defence and evolution of reversed sexual size dimorphism in snowy owls *Nyctea scandiaca*. *Ornis Scand* 14:58–62.
- Williams DL, Gonzalez Villavencio CM, Wilson S (2006): Chronic ocular lesions in tawny owls (*Strix aluco*) injured by road traffic. *Vet Rec* 159:148–153.
- Wink M, Heidrich P, Sauer-Gurth H, Elsayed AA, Gonzalez J (2008): Molecular phylogeny and systematics of owls (Strigiformes); in König C, Weick F (eds): *Owls of the World*. London, Christopher Helm, pp 42–63.
- Wood CA (1917): *The Fundus Oculi of Birds, Especially as Viewed by the Ophthalmoscope: A Study in Comparative Anatomy and Physiology*. Chicago, Lakeside Press.